© 2017. Published by The Company of Biologists Ltd | Development (2017) 144, 897-904 doi:10.1242/dev.146282

RESEARCH ARTICLE

Eccentric position of the germinal vesicle and cortical flow during oocyte maturation specify the animal-vegetal axis of ascidian embryos

Masumi Tokuhisa, Miyuki Muto and Hiroki Nishida*

ABSTRACT

The animal-vegetal (A-V) axis is already set in unfertilized eggs. It plays crucial roles in coordinating germ-layer formation. However, how the A-V axis is set has not been well studied. In ascidians, unfertilized eggs are already polarized along the axis in terms of cellular components. This polarization occurs during oocyte maturation. Oocytes within the gonad have the germinal vesicle (GV) close to the future animal pole. When the GVs of full-grown oocytes were experimentally translocated to the opposite pole by centrifugal force, every aspect that designates A-V polarity was reversed in the eggs and embryos. This was confirmed by examining the cortical allocation of the meiotic spindle, the position of the polar body emission, the polarized distribution of mitochondria and *postplasmic*/*PEM* mRNA, the direction of the cortical flow during oocyte maturation, the cleavage pattern and germ-layer formation during embryogenesis. Therefore, the eccentric position of the GV triggers subsequent polarizing events and establishes the A-V axis in eggs and embryos. We emphasize important roles of the cortical flow. This is the first report in which the A-V axis was experimentally and completely reversed in animal oocytes before fertilization.

KEY WORDS: Ascidians, Animal-vegetal axis, Germ layer, Oocyte maturation, Germinal vesicle, Localized maternal factors, *Halocynthia roretzi*

INTRODUCTION

The animal-vegetal (A-V) axis of eggs is called the primary axis and serves as a coordinate along which future germ layers are organized. In chordates, ectoderm, mesoderm and endoderm are arranged along the axis in this order (Lemaire et al., 2008). However, how the A-V axis is set during oogenesis and oocyte maturation has not been well studied. The animal pole of eggs is defined as the position that is close to the egg nucleus and less yolky cytoplasm, from which polar bodies are extruded during oocyte maturation. The vegetal pole is the opposite side and is enriched in yolk (Gilbert, 2014). On the other hand, in most invertebrate eggs, yolk granules are distributed evenly, and thus the positions of female nuclei and polar bodies have been regarded as a more universal morphological hallmark of the animal pole.

In the ascidian *Halocynthia roretzi*, cytoplasmic transfer experiments have shown that unfertilized eggs already have polarity in terms of tissue-forming activities (Nishida, 2005). Consistent with these findings, unfertilized ascidian eggs are polarized along the A-V axis in terms of cellular components such as mitochondria and localized maternal RNAs (Makabe and Nishida, 2012; Prodon et al., 2007; Sardet et al., 2005). Recent analyses have indicated that, in *Halocynthia* and *Ciona*, the polarized distribution of egg components is established during oocyte maturation (Prodon et al., 2006, 2008). In *Halocynthia*, the germinal vesicle (GV) is positioned close to the future animal pole where the polar bodies are released (Fig. 1A) (Prodon et al., 2008). Eccentric positioning of the GV close to the future animal pole is common in diverse animals from cnidarians and echinoderms to *Xenopus* (Freeman, 1987; Gard, 1993; Matsuura and Chiba, 2004). By translocating the GV, we reasoned that we might be able to reveal the causal relationship between the GV position and orientation of the future A-V axis. To this end, we took advantage of the eccentric position of the GV in *Halocynthia* and applied centrifugal force. The eccentric position of the GV before centrifugation enabled us to predict the future animal pole and mark the site.

Processes during oocyte maturation in *Halocynthia* have been observed in detail (Fig. 1Aa-d) (Prodon et al., 2008, 2009). Soon after GV breakdown (GVBD, Fig. 1Ab), a meiotic apparatus (MA) forms at the position of the GVBD, and the MA approaches the closest cortex (Fig. 1Ac). In GV oocytes, mitochondria (Fig. 1A, green line) and *postplasmic/PEM* mRNAs (e.g. *Pem* mRNA, red dots) are present in the entire cortex. After GVBD, they are gradually excluded from the animal pole region, resulting in a mitochondrial 'hole' and gradient distribution of *postplasmic/PEM* mRNAs, and eggs become polarized along the A-V axis (Fig. 1Aa-d). Concurrent with the movement of mitochondria and RNAs, cytoplasmic flow occurs (Fig. 1Ac, arrows), which flows downward from the animal pole in the cortical region. The plasma membrane also moves downward because particles attached to the oocyte surface moves downward (Prodon et al., 2008). Microfilaments and non-muscle myosin II ATPase, but not microtubules, are required for the flow. Relocation of RNAs and mitochondria is also sensitive to microfilament inhibitors, suggesting that the actin-driven cortical flow plays a role in exclusion of these cytoplasmic components from the animal pole (Prodon et al., 2006, 2008).

In the present study, the GVs of full-grown oocytes were experimentally translocated to the opposite pole by centrifugal force. In these GV-reversed oocytes, every aspect that designates A-V polarity mentioned above, as well as cleavage pattern and germ-layer formation during embryogenesis was reversed along the axis. Therefore, the eccentric position of the GV triggers subsequent polarizing events during oocyte maturation and establishes the A-V axis in eggs and developing embryos.

Department of Biological Sciences, Graduate School of Science, Osaka University, 1-1 Machikaneyama-cho, Toyonaka, Osaka 560-0043, Japan.

*Author for correspondence (hnishida@bio.sci.osaka-u.ac.jp)

H.N., 0000-0002-7249-1668

Received 28 October 2016; Accepted 11 January 2017

Development (2017) 144, 897-904 doi:10.1242/dev.146282

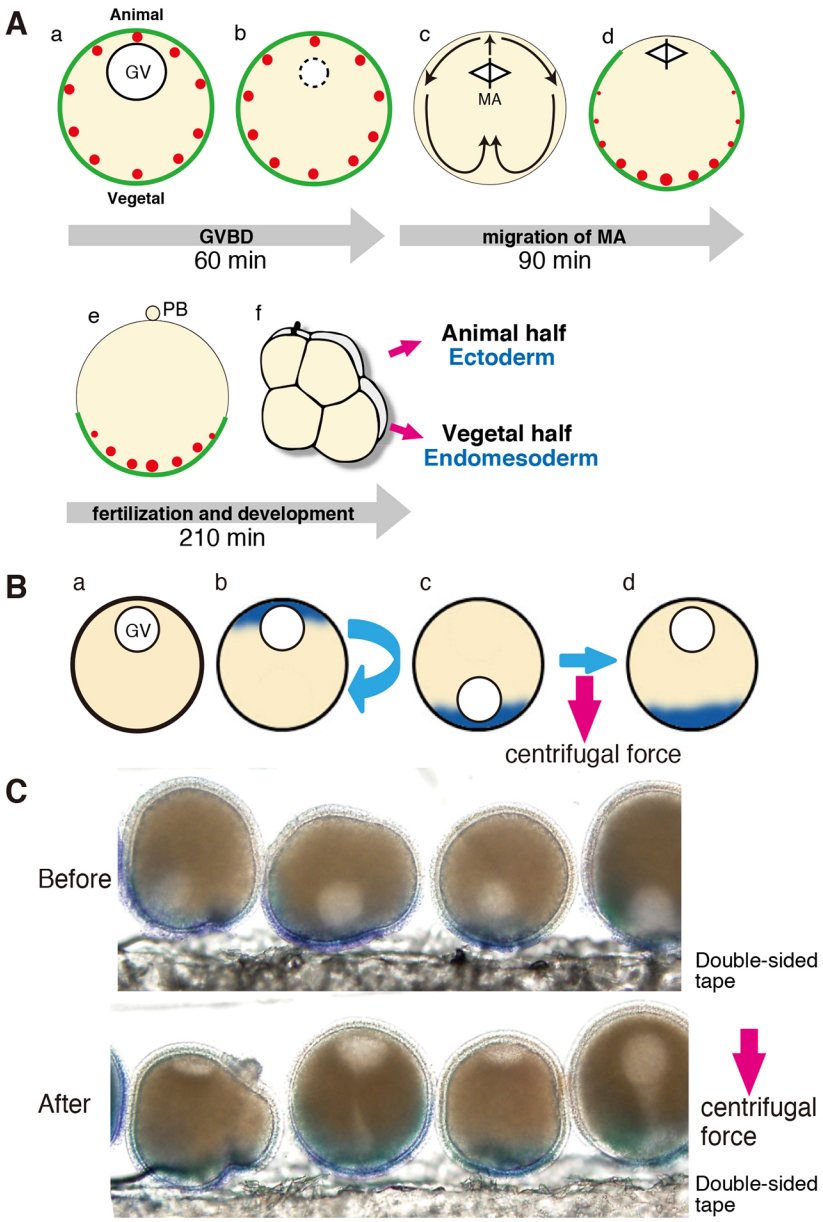

Fig. 1. Polarized events during oocyte maturation and embryogenesis, and experimental design. (Aa-f) Summary of events related to the A-V axis. The animal pole is upwards. The approximate time course is shown. Green lines represent the distribution of mitochondria; red dots indicate that of *postplasmic*/*PEM* mRNAs. Directions of the MA movement and cortical flow are shown by arrows. GV, germinal vesicle. GVBD, germinal vesicle breakdown. MA, meiotic apparatus. (Ba-d) The experimental design. The direction of centrifugal force is shown by the red arrow. The original GV side was marked by Nile Blue vital staining. The oocytes were then rotated upside down using a needle, so that the GV was positioned at the centrifugal side. The GV was translocated to the opposite side during centrifugation. (C) Oocytes in the centrifugation chamber before and after centrifugation corresponding to Bc and Bd. Original GV side is labeled with Nile Blue.

RESULTS

Translocation of the germinal vesicle by centrifugal force

Fully grown oocytes with the GV were dissected from gonads during the spawning season. The oocytes of *Halocynthia* are relatively large (280 µm) and enriched with yolk compared with most solitary ascidian species. Oocytes begin spontaneous maturation after suspension in seawater and transit to the mature state at the first meiotic metaphase in 2-3 h (Lambert, 2005). Naturally spawned eggs are arrested at meiotic metaphase I, and fertilization triggers further meiosis events involving emission of two polar bodies (Fig. 1Ad-f). The original GV side was marked by Nile Blue vital staining after mounting the oocytes in the chamber (Fig. 1B, Fig. S1). Then, the oocytes were rotated upside down by a needle, so that the GV was positioned at the centrifugal side (Fig. 1Bb,c). One side of a glass chamber with GV oocytes was vertically inserted onto the top of agar bedding in a centrifugation tube (Fig. S1).The GV was translocated to the opposite side during centrifugation, but the oocyte did not rotate because the blue mark remained in the centrifugal side of the GV-reversed oocytes (Fig. 1C). In some oocytes after centrifugation (shown in Fig. 1C), the trajectory of the GV movement was recognized as a line of clear cytoplasm. So the GV likely moved linearly to the opposite side through the center of oocytes. The specific density of the GV is likely lighter than that of yolk-rich cytoplasm. Therefore, the GV moved to the centripetal side. The cytoplasm was not stratified by the applied centrifugal force. In addition to uncentrifuged controls, in centrifuged controls, oocytes were not rotated upside down by skipping the step shown in Fig. 1Bb,c, so that the GV is oriented toward the centripetal side and the GV does not move and stays in the original position during centrifugation.

Polar body emission and migration of the meiotic apparatus

The polar body is a readily recognizable hallmark of the animal pole after fertilization (Fig. 1Ae). If the site of polar body emission in GV-reversed oocytes is unaltered, the animal pole is predetermined in the cortex of the GV-oocyte independently of

Development (2017) 144, 897-904 doi:10.1242/dev.146282

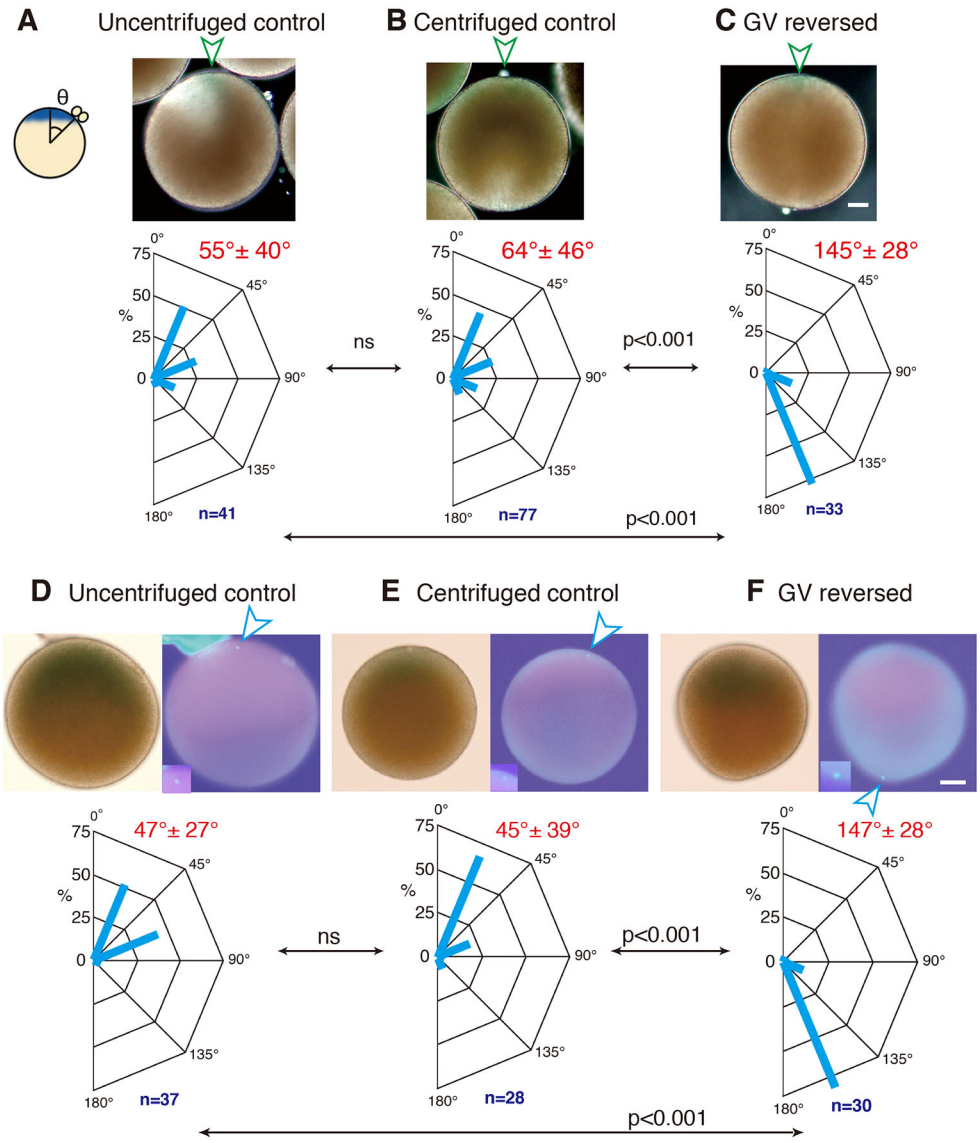

Fig. 2. Positions of the polar body and meiotic apparatus. (A-C) Polar body emission after fertilization and its angle (Θ) to the center of the blue-stained area (arrowheads) in uncentrifuged controls (A), centrifuged controls (B) and GV-reversed (C) oocytes. The original GV position is indicated by an arrowhead. (D-F) Positions of the meiotic apparatus (MA) in mature oocytes were visualized by DNA staining with DAPI (arrowheads). Nile Blue also emits red fluorescence under UV illumination. Insets are magnified views of the MA. Angles between the MA and center of the Nile Blue mark are shown underneath. The angles were scored every 45°. Data are mean±s.d. n, number examined. Statistical significance (chi-square test or Fisher's exact test) is shown. ns, not significant. Scale bar: 50 µm.

the position of the GV. If the site of polar body emission is reversed, the position of the GV specifies the animal pole. We measured angles between the center of the blue area (original GV position) and the site of polar body emission. The centers of the blue areas are oriented upwards in Fig. 2A-C (arrowheads). The angles were scored every 45°. In uncentrifuged oocytes and in centrifuged control oocytes, polar bodies tended to be emitted from the original animal pole that was stained with average angles of 55° and 64°, respectively. The averages can range from 22.5° to 157.5° in this type of scoring, but not from 0° to 180°. Every GV-reversed oocyte emitted a polar body. The polar body was present in the opposite side of the blue area, indicating that the polar bodies were emitted from the original vegetal pole. The differences between controls and GV-reversed oocytes were significant.

The position of the MA in mature but unfertilized eggs (Fig. 1Ad) was examined by visualizing DNA with 4,6-diamidino-2-phenylindole (DAPI). In addition to blue staining, Nile Blue emits red fluorescence under ultraviolet (UV) illumination (Fig. 2D-F). In contrast to the controls, the MA was positioned at the original vegetal pole in GV-reversed oocytes. This is consistent with the result of polar body emission and indicated that the MA moved toward the closest cortex after GVBD in both normal and GV-reversed oocytes. Therefore, the animal pole is not predetermined in the cortex before GVBD, and the position of the GV and subsequent allocation of the meiotic spindle define the animal pole.

Exclusion of mitochondria and maternally localized RNA from the animal pole

We examined whether redistribution of mitochondria (Fig. 1A, green line) and *postplasmic/PEM* mRNAs (e.g. *Pem* mRNA, Fig. 1A, red dots) is reversed in GV-reversed oocytes. Mitochondria were visualized by green fluorescence of the vital dye DiOC2(3) (Nishida, 1990; Zalokar and Sardet, 1984). The mitochondrial hole, which is present at the animal pole region in normal mature oocytes, is bordered by broken lines in Fig. 3A. We measured angle between the centers of Nile Blue staining and mitochondrial holes. Mitochondria were excluded from the animal pole in controls. By contrast, mitochondrial holes formed in the original vegetal hemisphere of GV-reversed oocytes. The differences between these observations were significant.

Development (2017) 144, 897-904 doi:10.1242/dev.146282

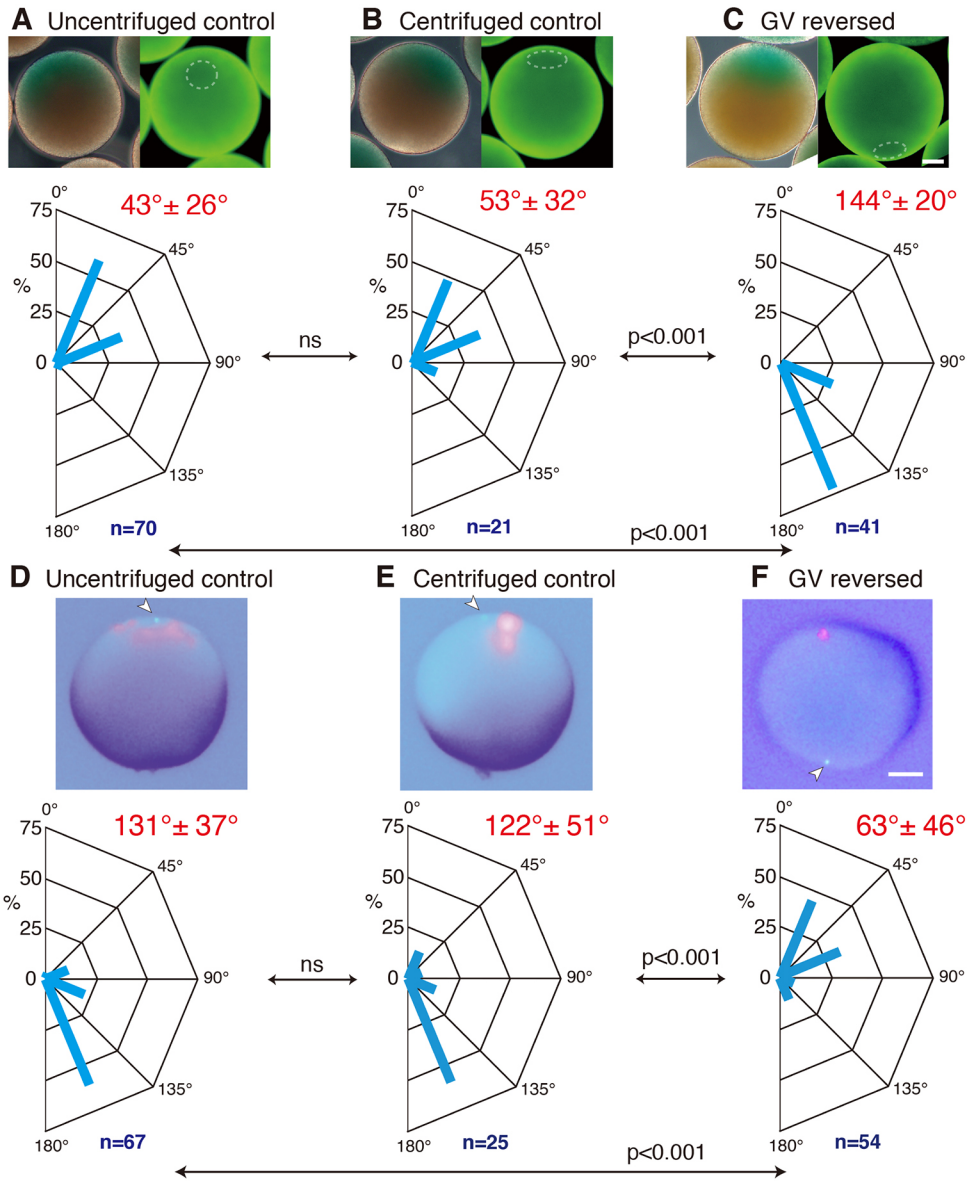

Fig. 3. Mitochondrial hole and localization of *Pem* mRNA. (A-C) (Left panels) Photos show the position of Nile Blue staining. (Right panels) Mitochondria in matured oocytes were vitally stained with DiOC2(3) (green). The mitochondrial hole is circled by the dashed line. (D-F) Distribution of *Pem* mRNA (dark blue) was detected by *in situ* hybridization. Red fluorescent beads were injected into the center of Nile Blue staining (original GV position) after fixation. The MA position is indicated by the arrowhead. Angles between the center of the *Pem* mRNA signal and red fluorescent beads are shown in the plots underneath. Data are mean±s.d. n, number examined. Statistical significance (chi-square test or Fisher's exact test) is shown. ns, not significant. Scale bar: 50 µm.

Pem is a *postplasmic/PEM* mRNA conserved between ascidian species (Makabe and Nishida, 2012; Yoshida et al., 1996). It is present as a gradient with its highest concentration at the vegetal pole in unfertilized ascidian eggs. *Pem* mRNA is anchored to the cortical endoplasmic network, just beneath the plasma membrane (Prodon et al., 2008; Sardet et al., 2003). Pem protein is involved in transcription quiescence in primordial germ cells. Pem sets the primordial germ cells aside from somatic cell differentiation programs and keeps the germ cells totipotent (Kumano et al., 2011; Shirae-Kurabayashi et al., 2011). It is also important for controlling unequal cell divisions at the posterior pole of the vegetal hemisphere in cleaving embryos (Negishi et al., 2007). Thus, unfertilized eggs are apparently polarized along the A-V axis in terms of functional molecules. The direction of *Pem* redistribution was also reversed in GV-reversed oocytes (Fig. 3D-F). In these oocytes, red fluorescent beads were injected into the center of the Nile Blue staining after fixation, because Nile Blue staining does not persist during *in situ* hybridization. Measurement of the angle between the fluorescent beads and the center of the *Pem* gradient showed significant differences between controls and GV-reversed oocytes. In the images shown in Fig. 3D-F, the MA position was also detected by DAPI staining (arrowheads), supporting that *Pem* mRNA distributes away from the MA position. Thus, the direction of mitochondria and *Pem* mRNA relocation was reversed in GV-reversed oocytes.

Cytoplasmic flow during oocyte maturation

Cytoplasmic flow (Fig. 1Ac, arrows) was recorded by time-lapse video microscopy of oocyte maturation (Movie 1). In the movies, movements of the clear cytoplasmic region, in which the MA is present (traced by the green line in the bottom middle oocytes), and the cortical flow can be visualized. In the centrifuged control, the cortical cytoplasm moved from the future animal pole towards the vegetal pole. In all six GV-reversed oocytes with successful recording of the flow, the clear cytoplasmic region approached the closest cortex, and the cortical flow apparently moved away from the eventual GV position after centrifugation. These results indicate an alteration in the direction of the cortical flow in GV-

Development (2017) 144, 897-904 doi:10.1242/dev.146282

reversed oocytes. We noticed that, in the oocyte shown in the bottom middle panel, the MA quickly reached the cortex (traced by the green line), but the cortical flow continued long after the MA movement. This finding would suggest that cortical flow is not only driven by MA movement, and that the actin cytoskeletons that preferentially reside in the cortex (Prodon et al., 2009) generate the driving force.

Cleavage pattern and cell fates

The cleavage pattern in ascidian embryos is stereotypical and conserved among ascidian embryos (Conklin, 1905; Nishida, 2005). Fig. 4A shows the animal and vegetal halves of a 16-cell embryo with the names of some relevant blastomeres. Each hemisphere is easily distinguishable by the remarkably unequal cell division in size, which generates B5.1 and B5.2 blastomeres at the posterior pole in the vegetal hemisphere. We made another mark at the center of Nile Blue staining by attaching a small oil droplet onto the plasma membrane, because the Nile Blue staining became ambiguous during the cleavage stages. Then, the location of the oil droplet was determined at the 16-cell stage (Fig. 4B,C). In control embryos, most oil droplets were located on cells of the animal hemisphere. By contrast, GV-reversed embryos preferentially contained oil droplets in the vegetal hemisphere, indicating reversal of the cleavage pattern along the A-V axis.

Germ-layer formation is tightly linked to the A-V axis. From the 4- to 8-cell stages, a cleavage furrow occurs horizontally and bisects

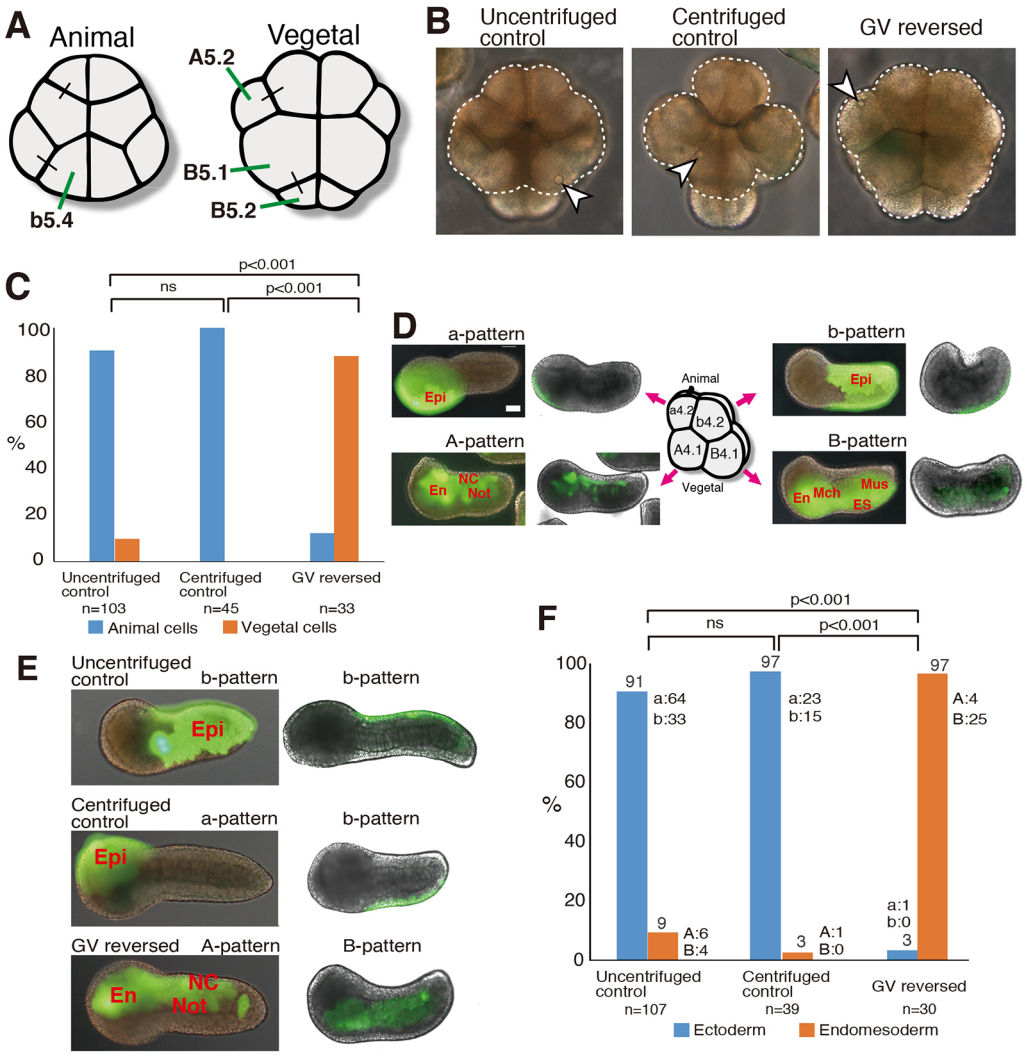

Fig. 4. Cleavage pattern and cell fate. (A) The arrangement of each blastomere in the animal and vegetal hemispheres of 16-cell embryos. Anterior is upwards. Bars connect sister blastomeres. Names of relevant cells are shown. B5.1 and B5.2 cells have divided unequally at the posterior pole in the vegetal hemisphere. (B) Three examples in which oil droplets (arrowheads) were attached to the original GV positions. Dashed lines indicate boundaries between animal and vegetal hemispheres. The droplets were on the animal blastomeres (b5.4) in the left and center images, whereas a droplet is on the vegetal cell (A5.2) in the right image. (C) Position of oil droplets in the animal (light blue) and vegetal (orange) hemispheres. Statistical significance (chi-square test or Fisher's exact test) is shown. ns, not significant. (D) Identified cells (e.g. a4.2) of an 8-cell embryos developed from dissected oocytes were labeled with a green fluorescent dye, neuro-DiO, resulting in a, b, A and B patterns of the descendants at the tailbud stage. Tailbud embryos were observed under a conventional fluorescence microscope (left) and confocal microscope (right). Dorsal is upwards. Embryos were not perfectly normal because they developed from dissected oocytes without vitelline membranes, mostly because of the failure of neural tube closure on the dorsal side. Epi, epidermis; En, endoderm; ES, endodermal strand; Mch, mesenchyme; Mus, muscle; NC, nerve cord; Not, notochord. (E) Examples of tailbud embryos developed from uncentrifuged controls, centrifuged controls and GV-reversed oocytes. (F) Results of cell fate tracing. Proportions of the a or b pattern (ectoderm, animal hemisphere origin, light blue), and A or B pattern (endomesoderm, vegetal hemisphere origin, orange) are shown. The number of specimens that showed each pattern is indicated on the right of the bars. Scale bar: 50 µm.

Development (2017) 144, 897-904 doi:10.1242/dev.146282

embryos into animal and vegetal hemispheres. Each blastomere of the 8-cell embryos can be unambiguously identified by its shape, position and texture. a4.2 and b4.2 are cells of the animal hemisphere, and A4.1 and B4.1 are those of the vegetal hemisphere (Fig. 4D). Animal cells mainly give rise to ectoderm, whereas vegetal cells develop into endomesoderm (Figs 1Af and 4D) (Nishida, 1987; Nishida and Satoh, 1983). Identified cells of 8-cell embryos developed from the dissected oocytes were labeled with a fluorescent lipophilic dye, neuro-DiO, and their descendants were observed at the tailbud stage by the green fluorescence. The results were consistent with the above-mentioned previous observations. The patterns of labeled cells were categorized into 'a', 'b', 'A' and 'B' patterns (named after the nomenclature of blastomeres of the 8-cell embryos, Fig. 4D). Some embryos were also observed under a confocal microscope to clearly identify whether labeled cells were present at the surface or inside of embryos (shown on the right of the conventional fluorescence images in Fig. 4D,E). The original position of the GV was then marked with Nile Blue followed by a small oil droplet mark. At the 8-cell stage, the blastomere with the oil droplet was marked with neuro-DiO to trace the cell fate (Fig. 4E,F). Control embryos showed the 'a' or 'b' pattern (ectoderm that is cell fate of the animal hemisphere, shown as light blue in Fig. 4F), whereas GV-reversed embryos had the 'A' or 'B' pattern (endomesoderm that is cell fate of the animal hemisphere, orange). These results indicate that the A-V axis was indeed reversed in terms of germ-layer formation during embryogenesis.

In conclusion, the eccentric position of the GV followed by the approach of the MA to the closest site of the cortex, as well as the flow of the cortical cytoplasmic away from the site of GVBD play important roles in establishment of the egg and embryonic A-V axis and in germ-layer formation of the ascidian.

DISCUSSION

In GV-reversed oocytes, every examined aspect that is polarized along the A-V axis of normal eggs and embryos was reversed. These aspects were: cortical allocation of the MA; the position of polar body emission; polarized mitochondria and *postplasmic/PEM* mRNA distributions; the direction of the cortical cytoplasmic flow during oocyte maturation; the cleavage pattern; and the future fate map in relation to germ-layer formation during embryogenesis. Our results indicate that the animal pole position is not predetermined in the cortex of GV oocytes, although the GV within the deep cytoplasm is located close to the cortical position that becomes the animal pole. The eccentric position of the GV and subsequent polarization processes, which are likely mediated by actin-driven cortical flow, establish the animal-vegetal axis in mature eggs, although there is a possibility that displacement of something other than the GV by centrifugation may be involved in the polarity reversal. This is the first report in which the A-V axis was experimentally and completely reversed in animal oocytes before fertilization.

The position of the GV has been translocated in several studies. In hydrozoans, the GV was mobilized to a random position by centrifugal force. It has been reported that polar bodies are released from the site of the relocated GV (Freeman, 1987). In starfish oocytes, the GV is located close to the future animal pole. The centrosomes are also anchored to the animal cortex. Even upon translocation of the GV, the centrosome remains at the animal cortex and consequently fails to emit the polar body (Matsuura and Chiba, 2004). In sea cucumbers, the GV initially resides in the center and then approaches the periphery, where the centrosomes are present, upon meiosis reinitiation. When the GV is moved to the future vegetal pole, it moves back to the cortex where the centrosomes are present (Miyazaki et al., 2005). Polar body emission was not examined in this study. In *Xenopus*, when the GV is moved to ectopic positions, the MA forms there and approaches the closest cortex. When the MA is located in the animal cortex, the polar body is released, whereas oocytes fail to emit the polar body when the MA is located in the vegetal cortex (Gard, 1993). These studies did not report the effects on polarized ooplasmic factor distribution or embryogenesis. Conveniently, in ascidians, and more generally in chordates, oocytes and MAs formed within oocytes do not have centrosomes or asters (Gard et al., 1995; Prodon et al., 2009; Szollosi et al., 1972). Therefore, the polar bodies were released even in GV-reversed oocytes that developed after fertilization.

In mice, oocyte maturation has been investigated extensively. Our results are reminiscent of studies using mouse oocytes. In mouse oocytes, the GV is located centrally. The MA forms at the center, and after random slow motion, the MA quickly approaches the closest cortex from a stochastically slightly off-center position (Schuh and Ellenberg, 2008; Verlhac et al., 2000; Yi et al., 2013) where the polar body is emitted. It has been proposed that the animal pole cortical site is randomly selected during MA relocation. This idea has been experimentally supported by the observation that the spindle changes its direction of relocation when it is artificially shifted to a new position (Schuh and Ellenberg, 2008). This observation is consistent with our findings because, in *Halocynthia*, the MA forms at the site of the eccentrically located GV and approaches the closest cortex. Interestingly, in the ascidian *Ciona*, the GV is positioned at the center of oocytes (Prodon et al., 2006), so the situation is more similar to that in mice. It is likely that, in chordates, the animal pole position is not predetermined in the cortex of GV oocytes, and is set as the site reached by the migrating MA approaches. The present results showed that this site not only specifies the site of polar body emission, but also has significant effects on the embryonic axis and germ-layer formation. They also suggest that cortical polarity of the mature oocyte plays crucial roles in establishment of the A-V axis of embryos.

The previous observation of ascidian oocyte maturation has emphasized the role of cortical flow. The *postplasmic/PEM* RNAs and mitochondria move in the same direction and with the same timing as the cortical flow. When the cortical flow is prevented by treatment with inhibitors of microfilaments and non-muscle myosin II ATPase, the *postplasmic/PEM* RNAs and mitochondria fail to move (Prodon et al., 2006, 2008). The present results further support the role of cortical flow in directing polarization of oocyte cortical components because the direction of the cortical flow was reversed in GV-reversed oocytes. What, then, determines the orientation and triggers the flow? MA migration is actin dependent in ascidians and mice. Cortical flow is also actin dependent in ascidians (Prodon et al., 2008). In mice, it has been proposed that a certain chromatin signal induces continuous reorganization of the cytoplasmic actin network nucleated by the Formin-2 and Arp2/3 complex (Schuh and Ellenberg, 2008; Yi et al., 2013). Similar mechanisms might also operate in ascidians. However, the entire cortex and plasma membrane also move in ascidian oocytes. Therefore, the actin network in the entire cortex would be remodeled and polarized. There is the possibility that GV contents, which are released in the animal pole region at GVBD, or factors tightly anchored to the GV surface could be involved in directing the flow orientation.

In the ovary, small yolk-less oocytes contain the GV in the center, whereas growing vitellogenic oocytes tend to have the GV eccentrically on the side opposite the attachment site to the

Development (2017) 144, 897-904 doi:10.1242/dev.146282

germinal epithelium (Prodon et al., 2008). This is the first manifestation of the A-V axis. We reconfirmed that this tendency is indeed correct, although there are many exceptions in which the GV is not located on the opposite side of the attachment site and, in some cases, the GV is located close to the attachment site. Possibly, oocytes tend to grow on the side close to the germinal epithelium, so that the GV is pushed away from the attachment site because oocytes of *Halocynthia* (280 µm) are larger than those of *Ciona* (130 µm). Consequently, the eccentric position of the GV determines the future animal pole during oocyte maturation in *Halocynthia*.

MATERIALS AND METHODS

Oocyte collection

Hermaphroditic adult *Halocynthia roretzi* were purchased from fishermen near the Asamushi Research Center for Marine Biology (Aomori, Japan) and the Onagawa Field Center (Miyagi, Japan). Whole gonads were dissected during the spawning season. Fully grown oocytes were aspirated from the ovary and incubated in Millipore-filtered (pore size: 0.2 µm) seawater containing 50 µg/ml streptomycin sulfate and 50 µg/ml kanamycin sulfate (Prodon et al., 2008). Oocytes begin spontaneous maturation after suspension in seawater and transit to the mature state at meiotic metaphase I in 2-3 h at 11-13°C (Prodon et al., 2008). If necessary, follicular cells were removed by incubation in seawater containing actinase E (crude protease, Kaken Pharmaceutical, Tokyo, Japan) for ∼5 min. In some cases, the vitelline membrane and surrounding follicular and test cells were removed by pipetting after enzymatic treatment with 1% thioglycolate and 0.05% actinase E at pH 10 for 15 min (Mita-Miyazawa et al., 1985; Prodon et al., 2008). Devitellinated oocytes were maintained in gelatin-coated dishes containing seawater. Polar bodies were observed after fertilization. Mature oocytes were fertilized and then devitellinated at 10 min after fertilization to clearly show the position of small polar bodies.

Centrifugation

The centrifugation method to translocate the GV was essentially performed according to the method developed for starfish by Matsuura and Chiba (2004). One side of a glass chamber with GV oocytes in it was vertically inserted onto the top of 3% agar bedding (30 ml) in a 50 ml centrifugation tube filled with seawater (Fig. S1A). The chambers were prepared manually as shown in Fig. S1B-D, consisting of two coverslips and spacers between them. The distance between the two coverslips was slightly shorter than the diameter of oocytes so that the chamber was able to hold the oocytes (Fig. S1D, see also Fig. 1C).

The original GV side was marked by spraying 1% Nile Blue (Wako, Osaka, Japan) in seawater using a micropipette after oocytes were inserted into the centrifugation chamber (Matsuura and Chiba, 2004). The oocytes were then rotated upside down by a needle, so that the GV was positioned at the centrifugal side (see Fig. 1B). The GV oocytes with follicular cells and the vitelline membrane were centrifuged at 2000 rpm (∼470 ***g***) for 15 min. Oocytes with the GV and Nile Blue mark on opposite sides to each other were selected after centrifugation as GV-reversed oocytes and used for further analysis. The GV was translocated to the opposite side during centrifugation, but the oocyte did not rotate because the blue mark remained in the centrifugal side in these GV-reversed oocytes. The cytoplasm was not stratified by the applied centrifugal force.

DNA and mitochondrial staining

The MA was detected by staining chromosomal DNA with 4,6-diamidino-2-phenylindole (DAPI). Devitellinated oocytes and eggs were fixed with 80% ethanol for 10 min and washed with PBS. The specimens were then mounted in VECTASHIELD mounting medium with DAPI (Vector Laboratories) and observed under UV illumination. Mitochondria were visualized by the green fluorescence of the vital dye DiOC2(3) (Molecular Probes) (Nishida, 1990; Zalokar and Sardet, 1984). Devitellinated live oocytes were incubated with 0.25 µg/ml DiOC2(3) for 20 min. The specimens were then observed under blue light illumination.

In situ hybridization

Detection of mRNA by whole-mount *in situ* hybridization was carried out using digoxigenin-labeled probes. The probes were detected conventionally using BCIP/NBT. *Harore-Pem* antisense RNA probes (*Hr-PEM*, GenBank Accession Number AB045129) were used to detect *Pem* mRNA (Negishi et al., 2007). Red fluorescent beads [FluoSpheres, carboxylate-modified microspheres, diameter 1.0 µm, red fluorescent (580/605), Thermo Fisher Scientific] were microinjected into the center of Nile Blue staining after fixation, because Nile Blue staining does not persist during *in situ* hybridization.

Measurement of angles

Angles between Nile Blue staining and the polar body/mitochondrial hole/*Pem* mRNA localization were measured under a binocular microscope (SMZ-18, Nikon). Oocytes were rotated so that they stayed in the proper orientation. The 180° degrees between both poles was divided into four sectors of 45° each. The angles were scored in every sector using the cross ocular micrometer as a reference. Angles between Nile Blue staining and the MA were measured using a conventional fluorescence microscope (BX61, Olympus). All data are expressed as the mean±s.d. The Chi-square test or Fisher's exact test was applied to assess significance. Results of at least three independent experiments were pooled for analysis.

Cell fate tracing

Mature oocytes were fertilized and then devitellinated 10 min after fertilization. A small silicon oil droplet was placed on the center of the plasma membrane stained with Nile Blue to mark the original GV side using a micropipette. This procedure was performed because Nile Blue staining became ambiguous during cleavage stages. Oil droplets were embedded in the plasma membrane and immobilized. The position of the oil droplet was determined at the 16-cell stage and scored for animal or vegetal locations. Occasionally, oil droplets were internalized together with cleavage furrows. Such specimens were discarded because it was difficult to determine the position precisely. In the cell fate tracing experiment, the blastomere with the oil droplet was identified at the 8-cell stage, and the blastomeres were fluorescently labeled with a lipophilic dye, Neuro-DiO (2 mg/ml, diluted in canola oil; Life Technologies) (Lambert et al., 2015; Shirae-Kurabayashi et al., 2006), using a micropipette. Descendants of the labeled blastomeres were determined at the tailbud stage under a conventional fluorescence microscope (BX61, Olympus) or a confocal microscope (LSM710, Zeiss). Neuro-DiO emits green fluorescence, so it was not interfered with by the red fluorescence of Nile Blue. However, diffusion of Neuro-DiO is slower than that of DiI. Therefore, the fluorescent intensity sometimes varied among the descendant cells of single blastomeres in 8-cell embryos.

To support normal development of devitellinated eggs, embryos were cultured in seawater supplemented with the supernatant of an egg homogenate (Nishida and Satoh, 1985). This seawater improved the rate of normal development of naked eggs, but eggs matured from dissected oocytes still showed slight developmental abnormalities, mostly due to the failure of neural tube closure. They gastrulated normally but ceased neural tube closure midway, resulting in a dorsally bending tail. Even in these embryos, tissue organization was normal and each tissue was identified unambiguously.

Time-lapse video recording

About 10 defolliculated oocytes with the vitelline membrane and accessory test cells within it were mounted, and their maturation processes were recorded by differential interference contrast microscopy at high resolution (4080×3072 pixels). The movie was recorded in 30 s intervals for a total of 2 h. The first two and last two frames were acquired in RGB color to show the position of Nile Blue staining, whereas the others were recorded in gray scale. Images were processed using ImageJ. Each oocyte that was recorded in the proper orientation was trimmed, and the brightness and contrast were adjusted to clearly show the cortical flow. One in every three frames was used to generate the final movies with a frame rate of 30 frames per second to reduce the file size and increase the speed of movies. Trajectory of MA movement was traced using the plug-in 'manual tracking' of ImageJ.

Acknowledgements
We thank the members of the Asamushi Research Center for Marine Biology and the Onagawa Field Center for help with collecting live ascidian adults, and the Seto Marine Biological Laboratory for help with their maintenance.

Competing interests
The authors declare no competing or financial interests.

Author contributions
H.N. and M.T. conceived the study. H.N. directed the study. M.T. conducted most experiments. M.T. and H.N. wrote the manuscript. M.M. contributed to initial optimization of the experimental set up for centrifugation.

Funding
This work was supported by Grants-in-Aid from the Japan Society for the Promotion of Science (22370078, 15H04377) and the Ministry of Education, Culture, Sports, Science, and Technology (23112714) to H.N.

Supplementary information
Supplementary information available online at
http://dev.biologists.org/lookup/doi/10.1242/dev.146282.supplemental

References

Conklin, E. G. (1905). The organization and cell lineage of the ascidian egg. *J. Acad. Nat. Sci.* **13**, 1-119.
Freeman, G. (1987). The role of oocyte maturation in the ontogeny of the fertilization site in the hydrozoan Hydractinia echinata. *Rouxs Arch. Dev. Biol.* **196**, 83-92.
Gard, D. L. (1993). Ectopic spindle assembly during maturation of Xenopus oocytes: evidence for functional polarization of the oocyte cortex. *Dev. Biol.* **159**, 298-310.
Gard, D. L., Affleck, D. and Error, B. M. (1995). Microtubule organization, acetylation, and nucleation in Xenopus laevis oocytes: II. A developmental transition in microtubule organization during early diplotene. *Dev. Biol.* **168**, 189-201.
Gilbert, S. F. (2014). *Developmental Biology*, 10th edn. Sunderland, MA: Sinauer Associates, Inc.
Kumano, G., Takatori, N., Negishi, T., Takada, T. and Nishida, H. (2011). A maternal factor unique to ascidians silences the germline via binding to P-TEFb and RNAP II regulation. *Curr. Biol.* **21**, 1308-1313.
Lambert, C. C. (2005). Signaling pathways in ascidian oocyte maturation: effects of various inhibitors and activators on germinal vesicle breakdown. *Dev. Growth Differ.* **47**, 265-272.
Lambert, W. S., Carlson, B. J., van der Ende, A. E., Shih, G., Dobish, J. N., Calkins, D. J. and Harth, E. (2015). Nanosponge-mediated drug delivery lowers intraocular pressure. *Transl. Vis. Sci. Technol.* **4**, 1.
Lemaire, P., Smith, W. C. and Nishida, H. (2008). Ascidians and the plasticity of the chordate developmental program. *Curr. Biol.* **18**, R620-R631.
Makabe, K. W. and Nishida, H. (2012). Cytoplasmic localization and reorganization in ascidian eggs: role of postplasmic/PEM RNAs in axis formation and fate determination. Wiley interdisciplinary reviews. *Dev. Biol.* **1**, 501-518.
Matsuura, R. K. and Chiba, K. (2004). Unequal cell division regulated by the contents of germinal vesicles. *Dev. Biol.* **273**, 76-86.
Mita-Miyazawa, I., Ikegami, S. and Satoh, N. (1985). Histospecific acetylcholinesterase development in the presumptive muscle cells isolated from 16-cell-stage ascidian embryos with respect to the number of DNA replications. *J. Embryol. Exp. Morphol.* **87**, 1-12.
Miyazaki, A., Kato, K. H. and Nemoto, S. (2005). Role of microtubules and centrosomes in the eccentric relocation of the germinal vesicle upon meiosis reinitiation in sea-cucumber oocytes. *Dev. Biol.* **280**, 237-247.
Negishi, T., Takada, T., Kawai, N. and Nishida, H. (2007). Localized PEM mRNA and protein are involved in cleavage-plane orientation and unequal cell divisions in ascidians. *Curr. Biol.* **17**, 1014-1025.
Nishida, H. (1987). Cell lineage analysis in ascidian embryos by intracellular injection of a tracer enzyme. III. Up to the tissue restricted stage. *Dev. Biol.* **121**, 526-541.
Nishida, H. (1990). Determinative mechanisms in secondary muscle lineages of ascidian embryos: development of muscle-specific features in isolated muscle progenitor cells. *Development* **108**, 559-568.
Nishida, H. (2005). Specification of embryonic axis and mosaic development in ascidians. *Dev. Dyn.* **233**, 1177-1193.
Nishida, H. and Satoh, N. (1983). Cell lineage analysis in ascidian embryos by intracellular injection of a tracer enzyme. I. Up to the eight-cell stage. *Dev. Biol.* **99**, 382-394.
Nishida, H. and Satoh, N. (1985). Cell lineage analysis in ascidian embryos by intracellular injection of a tracer enzyme. II. The 16- and 32-cell stages. *Dev. Biol.* **110**, 440-454.
Prodon, F., Chenevert, J. and Sardet, C. (2006). Establishment of animal-vegetal polarity during maturation in ascidian oocytes. *Dev. Biol.* **290**, 297-311.
Prodon, F., Yamada, L., Shirae-Kurabayashi, M., Nakamura, Y. and Sasakura, Y. (2007). Postplasmic/PEM RNAs: a class of localized maternal mRNAs with multiple roles in cell polarity and development in ascidian embryos. *Dev. Dyn.* **236**, 1698-1715.
Prodon, F., Sardet, C. and Nishida, H. (2008). Cortical and cytoplasmic flows driven by actin microfilaments polarize the cortical ER-mRNA domain along the a-v axis in ascidian oocytes. *Dev. Biol.* **313**, 682-699.
Prodon, F., Hanawa, K. and Nishida, H. (2009). Actin microfilaments guide the polarized transport of nuclear pore complexes and the cytoplasmic dispersal of Vasa mRNA during GVBD in the ascidian Halocynthia roretzi. *Dev. Biol.* **330**, 377-388.
Sardet, C., Nishida, H., Prodon, F. and Sawada, K. (2003). Maternal mRNAs of PEM and macho 1, the ascidian muscle determinant, associate and move with a rough endoplasmic reticulum network in the egg cortex. *Development* **130**, 5839-5849.
Sardet, C., Dru, P. and Prodon, F. (2005). Maternal determinants and mRNAs in the cortex of ascidian oocytes, zygotes and embryos. *Biol. Cell* **97**, 35-49.
Schuh, M. and Ellenberg, J. (2008). A new model for asymmetric spindle positioning in mouse oocytes. *Curr. Biol.* **18**, 1986-1992.
Shirae-Kurabayashi, M., Nishikata, T., Takamura, K., Tanaka, K. J., Nakamoto, C. and Nakamura, A. (2006). Dynamic redistribution of vasa homolog and exclusion of somatic cell determinants during germ cell specification in *Ciona intestinalis*. *Development* **133**, 2683-2693.
Shirae-Kurabayashi, M., Matsuda, K. and Nakamura, A. (2011). Ci-Pem-1 localizes to the nucleus and represses somatic gene transcription in the germline of *Ciona intestinalis* embryos. *Development* **138**, 2871-2881.
Szollosi, D., Calarco, P. and Donahue, R. P. (1972). Absence of centrioles in the first and second meiotic spindles of mouse oocytes. *J. Cell Sci.* **11**, 521-541.
Verlhac, M.-H., Lefebvre, C., Guillaud, P., Rassinier, P. and Maro, B. (2000). Asymmetric division in mouse oocytes: with or without Mos. *Curr. Biol.* **10**, 1303-1306.
Yi, K., Rubinstein, B., Unruh, J. R., Guo, F., Slaughter, B. D. and Li, R. (2013). Sequential actin-based pushing forces drive meiosis I chromosome migration and symmetry breaking in oocytes. *J. Cell Biol.* **200**, 567-576.
Yoshida, S., Marikawa, Y. and Satoh, N. (1996). Posterior end mark, a novel maternal gene encoding a localized factor in the ascidian embryo. *Development* **122**, 2005-2012.
Zalokar, M. and Sardet, C. (1984). Tracing of cell lineage in embryonic development of Phallusia mammillata (Ascidia) by vital staining of mitochondria. *Dev. Biol.* **102**, 195-205.